Evaluation of PEG-*b*-polycarbonates self-assemblies containing azobenzene or coumarin moieties as nanocarriers using paclitaxel as a model hydrophobic drug

Alejandro Roche[a,b], Violeta Morcuende-Ventura[a,b], Rosa M. Tejedor[c], Luis Oriol[a,b], Olga Abian[d,e,f,g,h]*, and Milagros Piñol[a,b]*

[a]*Instituto de Nanociencia y Materiales de Aragón (INMA), CSIC-Universidad de Zaragoza, Zaragoza 50009, Spain;* [b]*Departamento de Química Orgánica, Facultad de Ciencias, Universidad de Zaragoza, Zaragoza 50009, Spain;* [c]*Centro Universitario de la Defensa, Academia General Militar, Ctra. de Huesca s/n, 50090 Zaragoza, Spain;* [d]*Institute of Biocomputation and Physics of Complex Systems (BIFI), Joint Units IQFR-CSIC-BIFI and GBsC-CSIC-BIFI, Universidad de Zaragoza, Zaragoza, 50018, Spain;* [e]*Instituto Aragonés de Ciencias de la Salud (IACS), 50009, Zaragoza, Spain;* [f]*Instituto de Investigación Sanitaria Aragón (IIS Aragón), 50009, Zaragoza, Spain;* [g]*Centro de Investigación Biomédica en Red en el Área Temática de Enfermedades Hepáticas y Digestivas (CIBERehd), 28029, Madrid, Spain:* [h]*Departamento de Bioquímica y Biología Molecular y Celular, Universidad de Zaragoza, 50009, Zaragoza, Spain*

Contact: oabifra@unizar.es (O.A.); mpinol@unizar.es (M.P.)

Evaluation of PEG-b-polycarbonates self-assemblies containing azobenzene or coumarin moieties as nanocarriers using paclitaxel as a model hydrophobic drug

Aim: The work assesses the performance of nanocarriers from amphiphilic block copolymers with functional azobenzene or coumarin moieties for delivery of paclitaxel.

Methods: Placlitaxel was encapsulated by the nanoprecipitation method. Characterizations were performed by DLS, TEM, Zeta potential and HPLC. Cell viability was investigated in HeLa and Huh-5-2-cell lines.

Results: Coumarin-containing polymeric micelles (D_h = 26±2 nm, PDI = 0.28, ζ = –22.9±3.6 mV) with 11.2±0.5 %w/w drug loading showed enhanced cytotoxicity in HeLa cells (IC50 < 0.02 nM) compared to free paclitaxel (IC50 = 0.17±0.02 nM). Azobenzene-containing polymeric vesicles (D_h = 390±20 nm, PDI = 0.24, ζ = –33.2±5.0 mV) with a 6.8±0.4 %w/w drug loading showed increased cytotoxicity under 530 nm light (IC50 = 0.0114±0.00033 nM) in HeLa cells due to a stimulated delivery of paclitaxel.

Conclusion: Effectivity of these block copolymers as paclitaxel nanovectors and light stimulated release has been demonstrated.

Keywords: block copolymers; self-assembly; nanocarriers; drug loading; paclitaxel; light-stimulated.

1. Introduction

In last years, amphiphilic block copolymers (BCs) consisting of hydrophobic and hydrophilic polymeric segments have been considered ideal candidates for transport and delivery of therapeutic agents to improve their usually poor solubility and stability in aqueous media, to prolong their circulation time and to achieve their controlled and sustained release providing improved therapeutic profiles and minimising toxic side effects (Liu *et al*. 2006; Tyrrel *et al.* 2010; Ahmad *et al.* 2014; Hwang *et al.* 2020).

Depending on structural factors, amphiphilic BCs are able to self-associate in aqueous media forming nanometric size assemblies of different morphology, among which stand out core-shell micelles, which are capable of solubilising hydrophobic molecules by physical entrapment inside the internal hydrophobic core, and vesicles, which are larger in size than micelles and might locate either hydrophobic cargoes inside the membrane or hydrophilic cargoes in the aqueous inner lumen.

While poly(ethylene glycol) (PEG) is the habitual choice for the hydrophilic block for amphiphilic BCs, the hydrophobic block has been largely varied to either improve the drug loading capacity of the self-assemblies or to facilitate the drug sustained or controlled release. The hydrophobic block is selected to entrap hydrophobic cargoes in the self-assemblies and retard their release through molecular interactions, being hydrophobic interactions the most significant but also with the concurrence of additional drug-polymer interactions such as H-bond or π–π interactions to improve the loading capacity (Lv *et al.* 2018).

The applicability of these systems is enhanced by developing smart amphiphilic BC-based nanocarriers that are able to release the cargoes in response to an applied stimulus that causes the alteration of the self-assemblies. These stimuli responsive delivery systems are formulated by inserting in the amphiphilic BC units that are sensitive to light, changes in temperature, pH, redox or enzymatic activity, among others. From different stimuli, light is of particular interest because it can be externally applied in a non-invasive manner, easily controlling the dosing, time and space (Beauté *et al.* 2019). Light stimulated organic nanocarriers for on-demand drug delivery are mostly based on photoisomerisations or photoreactions promoted by UV. However, biomedical applications require of wavelengths with a higher penetration and low light-induced damage in biological tissues such as visible or NIR light (del Barrio *et al.*

2019). This is the case of massively used azobenzenes, whose response is based on their reversible light induced *E*-*Z* isomerisation and the usually concomitant changes on molecular geometry and polarity. In the majority of the proofs of concept, photoisomerisation of azobenzenes occurs under UV irradiation that limits extrapolation to *in vivo* drug delivery applications. Therefore, efforts in biomedical applications have been directed towards using visible light or NIR (Jerca and Hoogenboom 2018). Accordingly, tetra-*ortho* substituted azobenzenes have been designed and synthesised that can be photoisomerised with visible light (from blue to red). In particular tetra-*ortho*-methoxyazobenzenes can be reversible switched from *E*-to-*Z* in the visible range (Wegner 2012; Dong *et al.* 2015; Lieistner *et al.* 2021 Wu *et al.* 2016). NIR stimulated azobenzene isomerisation has also been achieved in an indirect way using up-converting nanoparticles (Weis and Wu 2018). Irreversible UV induced photocleavage of organic chromophores, such as *ortho*-nitrobenzyl, perylenylmethyl or coumarinyl esters, has also been used for drug delivery because it can provoke substantial local polarity changes in BC self-assemblies (Beauté *et al.* 2019). The cleavage can be stimulated by NIR irradiation (*via* two-photon absorption) as it has been demonstrated with micelles from amphiphilic BCs with coumarin polymethacrylates and polypeptides (Babin *et al.* 2009; Kumar *et al.* 2012).

Paclitaxel (PTX) is an anticancer agent effective for treatment of a wide spectrum of malignant tumours that has a water solubility of 1 μg mL^{-1}. This highly hydrophobic drug is often used as a model to explore the potential of nanocarriers in drug delivery applications because it requires suitable delivery vehicles for efficient administration (Barbuti and Chen 2015). In this sense, amphiphilic BCs have been shown to increase the water solubility of PTX also resulting in increased efficiency (Gothwal *et al.* 2016). A relevant example are poly(ethylene glycol)-*b*-poly(*D*,*L*-

lactide) (PEG-*b*-PDLLA) copolymer micelles, allowing drug loadings up to 25% w/w, that provide a high increase in the water solubility of PTX compared to conventional formulation of this drug, Taxol®, and that have been introduced into the market as Genoxol® PM (Liu *et al.* 2006; Zhang *et al.* 1996). Nevertheless, issues such as maximising the drug loading capacity, stability or therapeutic performance of the drug loaded self-assemblies are behind the design of a large variety of amphiphilic BCs that have been tested as polymeric delivery systems for PTX. Illustrative examples include changes on the structural composition of the hydrophobic block to increase the molecular interactions (Shi *et al.* 2015), or the use of dendritic hydrophobic blocks (Xiao *et al.* 2009) or miktoarm polymers (Li *et al.* 2010).

We have recently described different series of amphiphilic BCs consisting of a PEG segment and a hydrophobic aliphatic polycarbonate segment with either azobenzene or coumarin pendant functional moieties, which provide light-responsiveness (Figure 1) (Roche *et al.* 2019; Roche *et al.* 2020). We considered the use of aliphatic polycarbonates in amphiphilic BCs as they represent hydrolytically degradable biocompatible materials opposite for instance to vinyl polymers with extremely low degradation profiles (Dai and Zhang 2017; Brannigan and Dove 2017). Also, aliphatic polycarbonates can be precisely prepared in terms of molar mass and structure by ring opening polymerisation (ROP) from cyclic carbonates with chemical handles affording highly versatile polymer platforms where appropriate functionalization post-polymerization can provide additional light responsiveness (Becker and Wurm 2018). Therefore, we have previously demonstrated that vesicles self-assembled from azobenzene-containing PEG-*b*-polycarbonates are able to release loaded hydrophobic or hydrophilic fluorescent probes when irradiated, due to the molecular mobility and polarity changes induced by the reversible *E*-*Z*

photoisomerisation of the azobenzene. In the case of micelles self-assembled from coumarin-containing PEG-*b*-polycarbonates, light also promotes the release of loaded fluorescent probes because of a polarity change associated to the irreversible photocleavage of the coumarin ester (Roche *et al.* 2019; Roche *et al.* 2020). Encouraged by these preliminary results, here, we have here explored the potential as drug nanocarriers of these azobenzene vesicles and coumarin-containing micelles by screening the drug loading and release properties using PTX as a hydrophobic drug model.

2. Materials and methods

2.1. Materials

The synthesis, characterisation and self-assembly in water of the investigated BCs, PEG_{2k}-*b*-PC(AzoOMe) and PEG_{5k}-*b*-PC(Cou) (Figure 1) have been earlier described (Roche *et al.* 2019; Roche *et al.* 2020). These amphiphilic BCs consist of a PEG hydrophilic segment of either 2 kDa or 5 kDa average molar mass, and a polycarbonate hydrophobic block that provides a biodegradable backbone. In short, BCs with defined degrees of polymerisation and narrow molar mass distributions were synthesised by combining the organocatalysed ROP of a 2,2-di(hydroxymethyl)propionic acid (bis-MPA)-based cyclic carbonate with alkyne pendant groups and a post-polymerisation modification by copper(I) catalysed azide-alkyne cycloaddition (CuAAC). Accordingly, ROP of the propargyl 2,2-di(hydroxymethyl)propionate cyclic carbonate using methyl ether poly(ethylene glycol) as the macroinitiator and 1,8-diazabicyclo(5,4,0)undec-7-ene/1-(3,5-bis(trifluoromethyl)phenyl)-3-cyclohexylthiourea as the catalytic system rendered a BC with alkyne side groups on the polycarbonate segment that were subsequently subjected to a CuAAC post-

functionalisation with the corresponding azobenzene or coumarin azides. Self-assembly of PEG_{2k}-*b*-PC(AzoOMe) and PEG_{5k}-*b*-PC(Cou) was promoted by the co-solvent method using the THF/water solvents pair. Stability and morphology of the self-assembled structures were determined by critical aggregation concentration (CAC), dynamic light scattering (DLS) and transmission electron microscopy (TEM).

2.2. Preparation and morphological characterisation of PTX loaded self-assemblies

Milli-Q® water (1.5 mL) was gradually added to a solution of the BC (5 mg) and PTX (0.6, 1.2 or 2.4 mg) in spectroscopic grade THF (1 mL) previously filtered through a 0.2 μm polytetrafluoroethylene (PTFE) filter. The self-assembly process was followed by measuring the loss of transmitted light intensity at 650 nm due to scattering as a function of water content. When a constant value of turbidity was reached, the resulting suspension was filtered through a 5 μm cellulose acetate filter and dialysed against water using a Spectra/Por^{TM} dialysis membrane (MWCO, 1 kDa) for 2 days to remove THF, changing water 3 times. The dialysed suspensions were then filtered again to remove the non-encapsulated solid PTX from the self-assemblies dispersions with either a 5.0 μm cellulose acetate filter for PEG_{2k}-*b*-PC(AzoOMe) vesicles or 0.45 μm cellulose acetate filter PEG_{5k}-*b*-PC(Cou) micelles. The filter was selected according to the size of the self-assemblies to be filtered.

Particle size, given as the hydrodynamic diameter (D_h), and particle size distribution (PDI) were determined by dynamic light scattering (DLS) using self-assemblies dispersions of 0.10 mg mL^{-1} concentration. Measurements were carried out in a Malvern Instrument Nano ZS using a He-Ne laser with a 633 nm wavelength and a detector angle of 173° at 25 °C. Zeta potential (ζ) was determined using a Folded

Capillary Zeta Cell DTS1070. All values were given as an average of three measurements on each sample to ensure reproducibility (n=3).

Morphology of the self-assemblies was studied by transmission electron microscopy (TEM) using a TECNAI G20 (FEI Company) electron microscope operating at 200 kV. 10 μL of a 1.0 mg mL^{-1} self-assemblies water dispersion was deposited onto carbon coated copper grid and the water removed by capillarity using filter paper. The samples were stained with uranyl acetate removing the excess by capillarity using filter paper. The grids were dried overnight under vacuum.

2.3. Determination of PTX concentration by HPLC

PTX concentration in the aqueous self-assemblies dispersions was determined by high performance liquid chromatography (HPLC) using a Waters 600 controller pump system with a mixture acetonitrile/water (1:1) as the mobile phase at a 1 mL min^{-1} flow rate, a column Waters Spherisorb 5μm C8 (4.6×250 mm, particle size 5 μm and pore size 80 Å) as stationary phase and a Waters 2998 PDA detector. In order to destroy the self-assemblies so that the PTX is released to the medium, the water suspension of PTX-loaded self-assemblies (250 μL) was diluted with acetonitrile (250 μL) and sonicated for 10 min, and then injected into the HPLC system. PTX quantification was carried out by analysing samples in triplicate at 227 nm wavelength in three independent experiments (n=9). From the obtained values, encapsulation efficiency (% EE given as %w/w) and drug loading (% DL given as %w/w) capacity were determined using the following equations 1 and 2:

$$\%\, EE \;=\; \frac{mass\ of\ encapsulated\ PTX}{mass\ of\ PTX\ in\ feed} \times 100 \qquad (1)$$

$$\%\, DL \;=\; \frac{mass\ of\ encapsulated\ PTX}{mass\ of\ PTX\text{-}loaded\ self\text{-}assemblies} \times 100 \qquad (2)$$

2.4. Cell culture and cytotoxicity assays

HeLa cells were grown in Dulbecco's modified Eagle's medium (DMEM) (Gibco™, ThermoFisher ES) supplemented with 1×non-essential amino acids (Gibco™), 100 IU mL^{-1} penicillin (Gibco™), 100 µg mL^{-1} streptomicin (Gibco™). Huh-5-2 cells were grown in Dulbecco's modified Eagle's medium (DMEM; Gibco™), supplemented with 1×non-essential amino acids (Gibco™), 100 IU mL^{-1} penicillin (Gibco™), 100 µg mL^{-1} streptomicin (Gibco™) and 250 µg mL^{-1} geneticin G418 (Gibco™).

HeLa or Huh-5-2 cell lines were seeded at a density of approximately 7×10^3 cells per well in a 96 well plate with a volume of 100 µL of DMEM (supplemented as described above). After 24 h, DMEM was removed and 100 µL of DMEM with serial dilutions of the tested compounds (PTX-loaded self-assemblies, free-PTX and unloaded self-assemblies) were added. Cells were allowed to proliferate at 5 %v/v CO_2 concentration and 37 °C for 72 h. Cell number was determined by CellTiter 96 Aqueous One Solution Cell Proliferation Assay (Promega). The experiments were repeated thrice and all evaluations were performed in triplicate (n=9). Cell viability data were analyzed with Origin program and fitted to the following mathematical function: $y = \frac{A_0 - A_f}{1+(\frac{x}{IC50})^{nh}} + A_f$ where A_0 is the maximal cell viability, A_f is the minimal cell viability, IC50 is the x value at 50 % cell viability and nh is the Hill Coefficient.

2.5. Cytotoxicity assays upon 530 nm light illumination

HeLa cell lines were seeded at a density of approximately 7×10^3 cells per well in a 96 well plate with a volume of 100 µL of DMEM (supplemented as described above). After 24 h, DMEM was removed and 100 µL of DMEM with serial dilutions of the tested com-pounds (PTX-loaded self-assemblies, free-PTX or unloaded self-assemblies) were added. After 24 h of incubation, the plates were illuminated with 530 nm light (irradiance in the sample 30 µW cm^{-2}) using a Mightex LCS-0530-15-22 high power

LED. Then, cells were allowed to proliferate at 5 %v/v CO_2 concentration and 37 °C for further 48 h. Cell number was determined by CellTiter 96 Aqueous One Solution Cell Proliferation Assay (Promega).

To discard any damaging effect of the light on the cell culture, the cell viability of HeLa cells under 530 nm irradiation was determined. HeLa cells were seeded at a density of approximately 7×10^3 cells per well in six 96 well plates with a volume of 100 µL of DMEM (supplemented as described above). After 24 h of incubation, half of the plates were illuminated with a 530 nm LED source (irradiance in the sample 30 µW cm^{-2}). After a total of 72 h of incubation, cell number was determined by CellTiter 96 Aqueous One Solution Cell Proliferation Assay (Promega). Cell viability was unaffected.

The experiments were repeated thrice and all evaluations were performed in triplicate (n=9). Cell viability data were analyzed with Origin program and fitted to the following mathematical function: $y = \frac{A_0 - A_f}{1+(\frac{x}{IC50})^{nh}} + A_f$ where A_0 is the maximal cell viability, A_f is the minimal cell viability, IC50 is the x value at 50% cell viability and nh is the Hill Coefficient.

3. Results and Discussion

3.1. Encapsulation of PTX in vesicles of azobenzene-containing PEG-b-polycarbonate

In preceding papers, we proved the loading and UV light induced release abilities of vesicles self-assembled from amphiphilic linear-dendritic BCs composed of a PEG, with an average molecular mass of 2 kDa linked to the 4th generation of a bis-MPA-based dendron as the hydrophobic block whose periphery was decorated with 4-isobutyloxyazobenzenes (Blasco *et al.* 2013a; Blasco *et al.* 2013b). Vesicles were

loaded with either hydrophobic Nile Red or hydrophilic Rhodamine B fluorescent probes which were released by exposing them to a low intensity UV lamp. The proof-of-concept was extended to the linear-linear counterparts consisting of a PEG and a hydrophobic aliphatic polycarbonate based also on the bis-MPA building block (Roche *et al.* 2019). The linear-linear version with 4-isobutyloxyazobenzene units pending from the polycarbonate block were used to prepare polymeric self-assemblies able to release fluorescent probes under UV light stimulation. Nonetheless, looking for more suitable wavelengths in bio-applications, 2,2′,5,5′-tetramethoxyazobenzene was used instead to obtain polymeric self-assemblies with which release of loaded molecular fluorescent probes was triggered by visible light of 530 nm wavelength (Roche *et al.* 2019). In particular, PEG_{2k}-*b*-PC(AzoOMe) self-assembled into vesicles, as inferred from cryo-TEM images, with an average hydrodynamic diameter (D_h) of 220 nm determined by DLS, and a CAC 33 μg mL^{-1} whose loading and releasing ability activated by visible light was demonstrated with molecular fluorescent probes. Therefore, we envisioned the potential of this candidate to fabricate light activated nanocarriers, so that *in vitro* studies with PTX were addressed.

PTX-loaded PEG_{2k}-*b*-PC(AzoOMe) vesicles were prepared starting from a solution of the BC and the drug in THF using a 1.2:5.0 w/w PTX/BC ratio. Water was slowly added to induce simultaneously the formation of vesicles and drug incorporation. Upon self-assembly, PTX should be physically entrapped within the hydrophobic membrane of the vesicle. The organic solvent was then removed by dialysis against water for 48 h, while the residual unloaded PTX was subsequently eliminated by filtration. Estimated PTX concentration was 115 ± 6 μg mL^{-1} (0.135 ± 0.007 μM) that it is higher than reported PTX solubility in water. Therefore, calculated % EE (Equation 1) was 28.8 ± 1.4 %w/w, with the final amount of PTX incorporated into the

vesicles, given as % DL (Equation 2), being 6.8 ± 0.4 %w/w. Dispersion was stable over 1 week. Zeta potential (ζ) of the PTX-loaded self-assemblies was measured as it might provide information about particle stability. The value determined, ζ = –33.2 ± 5.0 mV, points to a satisfactory stability of the dispersion by preventing interactions between highly negatively charged nanoparticles (Feng and Huang 2001). According to TEM images, PTX-loaded vesicles were self-assembled (Figure 2a). Besides, by DLS a notable increase in the D_h (from average 220 nm to 390 nm) and dispersity of particles size (PDI from 0.11 to 0.28) of the self-assemblies was observed after encapsulation of PTX in PEG_{2k}-*b*-PC(AzoOMe) when compared to plain vesicles. Physicochemical characterization of PEG_{2k}-*b*-PC(AzoOMe) vesicles is summarised in Table 1.

3.2. Cytotoxicity studies of PTX-loaded vesicles of azobenzene-containing PEG-b-polycarbonate and effect of light illumination

Unloaded and PTX-loaded PEG_{2k}-*b*-PC(AzoOMe) vesicles were evaluated for their cytotoxicity against HeLa cell line using CellTiter 96® Reagent for incubation times of 72 h. To have comparable data, the polymer concentration was the same for both sets of experiments. *i.e.* either with unloaded or PTX-loaded vesicles. Besides, results were contrasted with those obtained with free-PTX at the same PTX concentration. The results of cell viability studies are collected in Figure 3. Cell viability was almost unaffected by incubation with unloaded PEG_{2k}-*b*-PC(AzoOMe) vesicles as far as BC concentration was kept below 4 μg mL^{-1} (Figure 3a). However, at the same PTX concentration, PTX-loaded vesicles showed an enhanced cytotoxicity in comparison to free-PTX in all the range of concentrations studied (Figure 3b). Half cytotoxic concentration (IC50) defined as the PTX concentration that it is cytotoxic for half of the initial cell population (*i.e.* PTX concentration for which cell viability is 50%) was determined (Figure 3b). IC50 for free-PTX was 0.17 ± 0.02 nM ($p < 0.05$) whereas the

value for PTX-loaded vesicles was about eight times lower (Figure 3b). Therefore, PTX cytotoxicity against HeLa cells was enhanced by encapsulation into the self-assemblies so a lower concentration of PTX should be necessary if encapsulated to achieve the same effect than free PTX.

Experiments were reproduced in parallel by exposing the cell culture to light (Figures 3c y 3d) after proving the tolerance of cells to the irradiation conditions (530 nm, 30 μW cm^{-2}). Therefore, cells were first incubated for 24 h with either unloaded vesicles, PTX-loaded vesicles or free-PTX. Then, they were illuminated at 530 nm for 10 min and finally, incubated for additional 48 h. In this case, it was also observed that encapsulation increases the efficiency of the PTX over the cell death. However, what is truly remarkable is that at the same PTX concentration, and for low PTX concentrations, toxicity was improved by 530 nm light irradiation (Figure 4). By exposing the cells to 530 nm light, IC50 was 0.0114 ± 0.0003 nM ($p < 0.05$) for PTX-loaded self-assemblies, which is half of the IC50 value determined for the non-illuminated culture incubated with PTX-loaded self-assemblies. Because the effect of light was discarded in a previous control experiment (see Materials and Methods Section), the results infer that visible light stimulates the release of PTX as consequence of the photoinduced isomerisation of the azobenzene moieties located in the hydrophobic inner part of the vesicle membrane.

Majority of literature on light responsive BCs assemblies where light triggered release is demonstrated by drug release analysis using fluorescent probes or drugs rely on UV light stimulation. Eventually, some of the systems are tested *in vitro* with culture cell (Rapp and DeForest 2021) but UV light shows poor tissue penetration and phototoxicity. Shifting to NIR wavelengths, more suitable for biomedical applications, is difficult using pendant organic chromophores because the light response is based on

low efficient two-photon absorption process. Recently, NIR response has been assisted by using up-converting nanoparticles (Wu and Butt 2016) or photothermal transduction nanoparticles (Liu *et al.* 2019) that make more complex the design and preparation of these hybrid nanocarriers. Therefore, development of drug delivery systems based on organic units conjugated to BCs that respond to visible light, mainly green or red, is still an alternative of great interest (Rapp and DeForest 2020), where light triggered drug release on culture cells has been scarcely reported (Yap *et al.* 2020). In this context, PEG_{2k}-*b*-PC(AzoOMe) vesicles are valuable green light responsive nanocarriers.

3.3. Encapsulation of PTX in micelles of coumarin-containing PEG-b-polycarbonate

Recently, we described the synthesis an amphiphilic BC, PEG_{5k}-*b*-PC(Cou), containing a pendant [7–(diethylaminocoumarin)–4–yl]methyl ester unit as side functional group (Roche *et al.* 2020). This BC self-assembled into uniform micelles with mean D_h of approx. 22 nm as determined by DLS at a CAC of 32 μg mL^{-1}. The polymeric micelles that were used to encapsulate the hydrophobic fluorescent probe Nile Red showed little leakage by simple physical diffusion, but the ability to release the payload under light stimulation was demonstrated using UV and NIR light.

Motivated by the fact that for hydrophobic molecules, micelles show considerable higher drug loading efficiencies than vesicles (Chen *et al.* 2010), and taken into account that amphiphilic LDBCs with coumarin peripheral groups have been used to optimise drug loading capacity and stability of SN-38 by π-π stacking interactions, which is a highly efficient but also highly insoluble aromatic anticancer agent (Xu *et al.* 2015), the PTX loading ability of the micelles was investigated. In this case, PTX was physically entrapped into the core of the polymeric micelles during the self-assembly process of PEG_{5k}-*b*-PC(Cou), which was similar to the described for PEG_{2k}-*b*-

PC(AzoOMe). Different PTX/BC mass ratios were used ranging from 0.6:5.0 to 2.4:5.0 w/w and amount of loaded PTX was determined by HPLC.

Indeed, % EE and % DL values, calculated according to equations 1 and 2, generally depend on the initial amount of drug feed on the loading process. Consequently, it is common to use large excesses of drug to approach the maximum PTX loading capacity of the micelles in detriment of % EE. In this case % EE values about 40-50 %w/w were reached in all cases using moderate-to-low initial PTX/BC mass ratios in the self-assembly process. The amount of PTX incorporated into the micelles, given as % DL, was also dependent on the feed amount in the self-assembly process. DL was only about 6 %w/w at the lowest PTX/BC ratio attempted (0.6:5.0 w/w) but increased up about 21 %w/w at the highest PTX/BC ratio attempted (2.4:5.0 w/w). However, such highly loaded micelles ended up into a macroscopic precipitate within a few hours of their preparation, which indicates the stability of the micelles cannot be preserved at high PTX contents (Liu *et al.* 2006; Kohoria *et al.* 2002). Nevertheless, stable micellar suspensions, whose physicochemical characterization is summarised in Table 1, were obtained with % DL of 11.2 ± 0.5 %w/w when a 1.2:5.0 w/w ratio was initially feed, that corresponds to a % EE value of 46.8 ± 2.1%w/w. Therefore, by using these polymeric self-assemblies, PTX concentration in solution was increased up to 253 ± 11 μg mL^{-1} (0.296 ± 0.013 μM). By TEM, PTX–loaded spherical micelles were identified (Figure 2b) with no appreciable changes in particle size when compared to unloaded ones (28 nm and 26 nm, respectively) and negative zeta potential values, $\zeta = -22.9 \pm 3.6$ mV. Furthermore, much higher % DL was achieved in micelles compared to the vesicles of PEG_{2k}-*b*-PC(AzoOMe) when loaded under the same conditions (*i.e.* using a 1.2/5.0 w/w PTX/BC ratio) (Table 1). This % DL is not far from that of the commercial formulation Genoxol-PM®, a polymeric micellar formulation of

PEG-*b*-PDLLA with similar size micelles (20-50 nm) and a 16.7 %w/w PTX loading, approved by clinical use and marketed in some Asian countries (Bernabeu *et al.* 2017). PEG-*b*-PDLLA micelles with 25 %w/w PTX loading have been described but they lack of long term stability (Zhang *et al.* 1996). Comparable drug loading levels, up to 15%w/w, have been reported for PEG-*b*-polycarbonates functionalised with varying contents of cholesterol specifically designed for delivery of PTX also coming to PTX solubility values of approx. 200 μg mL^{-1} (Lee *et al.* 2012).

3.4. Cytotoxicity studies of PTX-loaded micelles of coumarin-containing PEG-b-polycarbonate

PTX-loaded PEG_{5k}-*b*-PC(Cou) micelles were evaluated for their cytotoxicity against HeLa and their activity contrasted with that of unloaded micelles and free-PTX. The results are collected in Figure 5a and 5b.

First, the effect of the BC was ascertained and, it was found that for unloaded PEG_{5k}-*b*-PC(Cou) micelles (*i.e.* without PTX) cell viability was only notably suppressed at BC concentrations above 5 μg·mL^{-1} (Figure 5a). Cell viability of HeLa cells against PTX-loaded PEG_{5k}-*b*-PC(Cou) micelles was evaluated for PTX concentrations ranging from 0.02 to 1.38 nM. For PTX concentrations below 0.4 nM, PTX-loaded PEG_{5k}-*b*-PC(Cou) micelles showed a much higher cytotoxicity than free-PTX at the same doses (Figure 5b). As mentioned above, IC50 for free-PTX was 0.17 ± 0.02 nM after 72 h incubation; whereas, the IC50 for encapsulated PTX was found to be below the lowest encapsulated PTX concentration studied, *i.e.* IC50 for PTX-loaded micelles was below 0.02 nM PTX concentration, which is more than ten times lower (Figure 5b). Therefore, when BC concentration was below 0.15 μg·mL^{-1} and at equivalent PTX doses, encapsulated PTX showed enhanced cytotoxicity compared to free-PTX. For instance, at approx. 0.02 nM PTX concentration (≈ 0.017 μg·mL^{-1}) cell

viability for PTX-loaded micelles was around 30% while for free-PTX was 100%. Because at this BC concentration unloaded micelles showed no cytotoxicity, *i.e.* BC was below 5 $\mu g \cdot mL^{-1}$, it can be deduced that the enhanced cytotoxicity of encapsulated PTX is due to a more effective delivery of PTX to the cells in comparison to free-PTX, and not by effect of cytotoxicity of copolymer. Such a large increase in cytotoxicity efficiency at significantly low PTX concentrations is remarkable when compared to published results for cholesterol-containing polycarbonate BCs (Lee *et al.* 2012).

Persuaded by these results, experiments were replicated with Huh-5-2 cells (Figures 5c and 5d). Huh-5-2 is a subline cell from Huh 7 Lunet hepatocellular carcinoma in which has been previously reported LD50 values for PTX much higher that the LD50 values exhibited in HeLa cells (Gagandeep *et al.* 1999; Peng *et al.* 2014). Therefore, we evaluate the effect of our micelles in these cells to further study their capability in compound cell bioavailability improvement. In this case, for Huh-5-2 cell line, unloaded PEG_{5k}-*b*-PC(Cou) micelles showed no cytotoxicity in almost all the range of BC concentration studied, from 0.16 to 10.5 μg/mL (Figure 5c). Again, PTX-loaded PEG_{5k}-*b*-PC(Cou) micelles showed a higher cytotoxicity in comparison to free-PTX in all the concentrations range studied, from 0.02 to 1.37 nM (Figure 6d). PTX-loaded PEG_{5k}-*b*-PC(Cou) had an IC50 of 0.18 ± 0.02 nM, while the IC50 of free-PTX was not detected in the range of concentration studied, being the highest concentration 1.37 nM (Figure 5d). This suggests that the same PTX dose provokes a greater cytotoxic effect when PTX is loaded on the micelles, which means that a higher concentration of compound is promoted in the cells.

3.5. Cell morphology assessment of PTX-loaded micelles of coumarin-containing PEG-b-polycarbonate

A time-lapse study in a bright-field microscope was performed at the same incubation conditions than those for the cell viability studies to compare the activity of PTX-loaded micelles and free-PTX. Images collected at different incubation times are shown in Figure 6 for HeLa cell line. Time lapse studies were performed at a PTX concentration of 0.02 nM that it is the concentration at which the difference in cell viability between encapsulated and free-PTX was greater. For PTX-loaded micelles, after 10 h of incubation the majority of the cells appeared detached from the plate, whereas after 20 h most of them seemed to be apoptotic. However, for free-PTX, after 40 h, most of cells were still attached to the flask and in good shape (Figure 6). Time lapse studies were also performed with Huh-5-2 cells at a PXT concentration of 0.17 nM. Due to their different morphology, differences were not as apparent for Huh-5-2 as for HeLa cell lines. Although, differences were observed after 20 and 40 h incubation times between encapsulated and free-PXT, as the number of detached cells is appreciable higher for the PXT-loaded micelles than for free-PXT. Again, the time lapse studies show an improved delivery of PXT to cells is observed when encapsulated.

The loading/release abilities under UV and NIR stimulation of the micelles evaluated using a fluorescent hydrophobic probe, Nile Red, have been reported in a previous paper (Roche *et al.* 2020). Here, the study of the light illumination of PTX-loaded micelles on the cell viability was unsuccessfully attempted. NIR photocleavage of the coumarin ester is achieved by a two-photon process, which is a low efficient process that requires of pulsed laser of high energy unaffordable at the time for *in vitro* cell assays. Hence, despite not being the optimal conditions for biomedical applications, *in vitro* test were attempted using UV light to evaluate the light triggered release of PTX from loaded micelles. PTX-loaded micelles were irradiated at 365 nm

(30 mW cm^{-2}) for 60 s using a Dynmax 200-EC lamp equipped with a glass filter. The conditions were established from experiments recorded with Nile Red loaded micelles, where after 100 s light exposure an abrupt decrease of emission was observed associated to the cargoes release. Analysis of the illuminated micelles by HPLC revealed decomposition of PTX. Besides, the death of cells was also observed after exposing the cell cultures to this short irradiation time.

5. Conclusions

It has been demonstrated that both vesicles self-assembled from PEG_{2k}-*b*-PC(AzoOMe) and micelles from PEG_{5k}-*b*-PC(Cou) are efficient nanocarriers for PTX, enhancing its solubility in water and improving its delivery to HeLa and Huh-5-2 cells. PEG_{2k}-*b*-PC(AzoOMe) and PEG_{5k}-*b*-PC(Cou) are no cytotoxic for the studied cell lines, at concentrations up to 5-6 μg mL^{-1}. However, when PTX-loaded micelles or vesicles were prepared, at subcytotoxic polymer concentrations, HeLa cell viability was efficiently decreased in comparison to free-PTX at the same concentration. Additionallt, the activity of PTX-loaded PEG_{5k}-*b*-PC(Cou) micelles has been confirmed when tested against Huh-5-2 that are more resistant to PTX than HeLa cells and for which micelles have been shown to be especially effective. Finally, vesicles derived from azobenzene-containing block copolymer PEG_{2k}-*b*-PC(AzoOMe), it has been demonstrated that illumination with visible light has improved cytotoxicity due to the light-stimulated delivery of PTX.

Acknowledgements

Authors would like to acknowledge the use of Servicio General de Apoyo a la Investigación-SAI, Universidad de Zaragoza and of Centro de Química y Materiales de Aragón-CEQMA, Universidad de Zaragoza-CSIC.

Disclosure statement

No potential conflict of interest was reported by the authors

Funding

This research was funded by the Ministerio de Economía y Competitividad (MINECO)-FEDER, Spain, under the project grant number MAT2017-84838-P (L.O., M.P., Programa Excelencia), Fondo Social Europeo and Gobierno de Aragon-FEDER (E47_17R and B25_17R, FEDER 2014-2020 "Construyendo Europa desde Aragón"), Fondo de Investigaciones Sanitarias from Instituto de Salud Carlos III and European Union (ERDF/ESF, "Investing in your future") (PI15/00663 and PI18/00349 to O.A.), Centro de Investigación Biomédica en Red en Enfermedades Hepáticas y Digestivas (CIBERehd) to O.A.

References

Ahmad, Z., *et al.*, 2014. Polymeric micelles as drug delivery vehicles. *RSC Advances,* 4 (33), 17028.

Babin, J., *et al.*, 2009. A New two-photon sensitive block copolymer nanocarrier. *Angewandte Chemie International Edition*, 48 (18) 3329-3332.

Barbuti, A.M. and Chen, Z.-S., 2015. Paclitaxel through the ages of anticancer therapy: exploring its role in chemoresistance and radiation therapy. *Cancers*, 7 (4), 2360-2371.

Beauté, L., *et al.*, 2019. Photo-triggered polymer nanomedicines: From molecular mechanisms to therapeutic applications. *Advanced Drug Delivery Reviews,* 138, 148-166.

Becker, G. and Wurm, F.R., 2018. Functional biodegradable polymers via ring-opening polymerization of monomers without protective groups. *Chemical Society Reviews*, 47 (20), 7739-7782.

Bernabeu, E., *et al.*, 2017. Paclitaxel: what has been done and the challenges remain ahead. *International Journal of Pharmaceutics*, 526 (1-2), 474-495.

Blasco, E., *et al.*, 2013a. Light induced molecular release from vesicles based on amphiphilic linear-dendritic block copolymers. *Polymer Chemistry*, 4 (7), 2246-2254.

Blasco, E., *et al.*, 2013b. Light responsive vesicles based on linear-dendritic block copolymers using azobenzene-aliphatic codendrons. *Macromolecules*, 46 (15), 5951-5960.

Brannigan, R.P. and Dove, A.P., 2017. Synthesis, properties and biomedical applications of hydrolytically degradable materials based on aliphtic polyesters and polycarbonates. *Biomaterials Science*, 5 (1), 9-21.

Chen, W., *et al.*, 2010. pH-Sensitive degradable polymersomes for triggered release of anticancer drugs: a comparative study with micelles. *Journal of Controlled Release*, 142 (1), 40–46.

Dai, Y. and Zhang, X., 2017. Recent developments of functional aliphatic polycarbonates for the construction of amphiphilic polymers. *Polymer Chemistry*, 8 (48), 7429-7437.

del Barrio, J., *et al.*, 2019. Light-controlled encapsulation and release enabled by photoresponsive polymer self-assemblies. In: Li, Q, ed. Photoactive functional soft materials: Preparation, properties, and applications. Wiley-VCH: Weinheim, Germany, 413-448.

Dong, M., *et al.*, 2015. Red-shifting azobenzene photoswitches for in vivo use. *Accounts of Chemical Research*, 48 (10), 2662-2670.

Feng, S.S. and Huang, G., 2001, Effects of emulsifiers on the controlled release of placlitaxel (Taxol®) from nanospheres of biodegradable polymers. *Journal of Controlled Release*, 71 (1), 53-79.

Gagandeep, S., *et al.*, 1999. Paclitaxel shows cytotoxic activity in human hepatocellular carcinoma cell lines. *Cancer Letters*, 136 (1), 109-118.

Gothwal, A., *et al.*, 2016. Polymeric micelles: Recent advancements in the delivery of anticancer drugs. *Pharmaceutical Research*, 33, 18-39.

Hwang, D., *et al.* 2020. Polymeric micelles for the delivery of poorly soluble drugs: From nanoformulation to clinical approval. *Advanced Drug Delivery Reviews*, 156, 80-118.

Jerca, V.V. and Hoogenboom, R., 2108. Photocontrol in complex polymeric materials: fact or illusion. *Angewandte Chemie International Edition*, 57 (27), 7945-7947.

Kohoria, F., *et al.*, 2002. Process design for efficient and controlled drug incorporation into polymeric micelle carrier systems. *Journal of Controlled Release*, 78 (1-3), 155-163.

Kumar, S., *et al.*, 2012. Near-infrared light sensitive polypeptide block copolymer micelles for drug delivery. *Journal of Materials Chemistry*, 22 (15), 7252-7257.

Lee, A.L.Z., *et al.*, 2012. The use of cholesterol-containing biodegradable block copolymers to exploit hydrophobic interactions for the delivery of anticancer drugs. *Biomaterials*, 33 (6), 1921-1928.

Li, Y., *et al.*, 2010. A novel size-tunable nanocarrier system for targeted anticancer drug delivery. *Journal of Controlled Release*, 144 (3), 314-323.

Lieistner, A.L., *et al.* 2021. Fluorinated azobenzenes switchable with red light. *Chemistry-A European Journal*, 27 (31), 8094-8099.

Liu, J., *et al.*, 2006. Formulation of drugs in block copolymer micelles: drug loading and release. *Current Pharmaceutical Design*, 12 (36), 4685-4701. DOI: 10.2174/138161206779026263

Liu, Y., *et al.*, 2019. Photothermal therapy and photoacoustic imaging via nanotheranostics in fighting cancer. *Chemical Society Reviews*, 48 (7), 2053-2108.

Lv, S., *et al.*, 2018. High Drug Loading and Sub-Quantitative Loading Efficiency of Polymeric Micelles Driven by Donor–Receptor Coordination Interactions. *Journal of the American Chemical Society*, 140, 1235-1238.

Peng, X., *et al.*, 2014. Autophagy promotes paclitaxel resistance of cervical cancer cells: involvement of Warburg effect activated hypoxia-induced factor 1-α-mediated signaling. *Cell Death and Disease*, 5, e1367.

Rapp, T.L. and DeForest C.A., 2020. Visible Light-responsive dynamic biomaterials: going deeper and triggering more. *Advanced Healthcare Materials*, 9 (7), 1901553.

Rapp, T.L. and DeForest C.A., 2021. Targeting drug delivery with light: a highly focused approach. *Advanced Drug Delivery Reviews*, 171, 94-107.

Roche, A., *et al.*, 2019. Polymeric self-assemblies based on tetra-ortho-substituted azobenzene as visible light responsive nanocarriers. *Polymers*, 11 (12), 206.

Roche, A., *et al.*, 2020. Supramolecular block copolymers as novel UV and NIR responsive nanocarriers based on a photolabile coumarin unit. *European Polymer Journal*, 126, 109561.

Shi, Y., *et al.*, 2015. Complete regression of xenograft tumors upon targeted delivery of paclitaxel via π-π stacking stabilized polymeric micelles. *ACS Nano*, 9 (4), 3740-3752.

Tyrrell, Z.L., *et al.*, 2010. Fabrication of micellar nanoparticles for drug delivery through the self-assembly of block copolymers. *Progress in Polymer Science*, 35 (9), 1128-1143.

Wegner, H.A., 2012. Azobenzenes in a new light-switching in vivo. *Angewandte Chemie International Edition*, 51 (20), 4787-4788.

Weis P. and Wu, S., 2018. Light-switchable azobenzene –containing macromolecules: from UV to Near Infrared. *Macromolecular Rapid Communications*, 39 (1), 1700220.

Wu, D., *et al.* 2016. A red-ligth azobenzene di-maleimide photoswitch: pros and cons. *Advanced Optical Materials*, 4 (9), 1402-1409.

Wu, S. and Butt, H.J., 2016. Near-Infrared-sensitive based on upconverting nanoparticles. *Advanced Materials*, 28 (6), 1208-1226.

Xiao, K., *et al.*, 2009. A self-assembling nanoparticle for paclitaxel delivery in ovarian cancer. *Biomaterials*, 30 (30), 6006-6016.

Xu, G., *et al.*, 2015. Functional-segregated coumarin-containing telodendrimer nanocarriers for efficient delivery of SN-38 for colon cancer treatment. *Acta Biomaterialia*, *21*, 85-98.

Yap, J.E., *et al.*, 2020. Visible light-responsive drug delivery nanoparticle via donor-aceptor Stenhouse adducts (DASA). *Macromolecular Rapid Communications*, 41 (21), 2000236.

Zhang, X., *et al.*, 1996. Development of amphiphilic diblock copolymers as micellar carriers of taxol. *International Journal of Pharmaceutics*, 132 (1-2), 195-206.

Table 1. Characterisation of PEG_{2k}-*b*-PC(AzoOMe) vesicles and PEG_{5k}-*b*-PC(Cou) micelles loaded with Paclitaxel) [a]

Polymer	Particle size (nm) ± SD [b]	Polydispersity index [b]	Zeta potential (mV) ± SD [c]	Encapsulation Efficiency (%w/w) ± SD [d]	Drug Loading (%w/w) ± SD [d]	PTX concentration (μg mL^{-1} [μM]) ± SD [d]
PEG_{2k}-*b*-PC(AzoOMe)	390 ± 20	0.28	– 33.2 ± 5.0	28.8 ± 1.4	6.8 ± 0.4	115 ± 6 [0.135 ± 0.007]
PEG_{5k}-*b*-PC(Cou)	26 ± 2	0.24	– 22.9 ± 3.6	46.8 ± 2.1	11.2 ± 0.5	253 ± 11 [0.296 ± 0.013]

[a] Paclitaxel-loaded self-assemblies were prepared from 1.2/5.0 mg/mg paclitaxel/block copolymer on the self-assembly process when using 1.0/1.5 mL/mL of tetrahydrofuran/water

[b] Particle size and particle size distribution given as the hydrodynamic diameter (D_h) and polydispersity index (PDI) determined by DLS. Data given as mean ± SD, n=3.

[c] Data given as mean ± SD, n=3.

[d] Paclitaxel (PTX) content in a 1 mg mL^{-1} polymer concentration solution. Data given as mean ± SD, n=9.

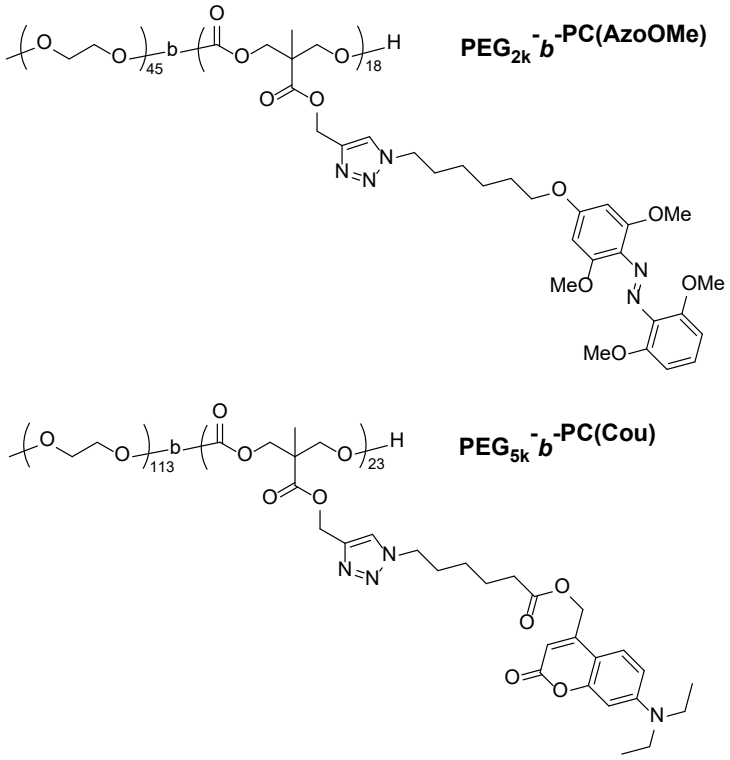

Figure 1. Chemical structure of the investigated poly(ethylene glycol)-*b*-polycarbonates (PEG-*b*-PC) containing light-responsive units, either 2,2′,5,5′-tetramethoxyazobenzene (AzoOMe) or [7–(diethylaminocoumarin)–4–yl]methyl ester (Cou) units, in the polycarbonate hydrophobic block.

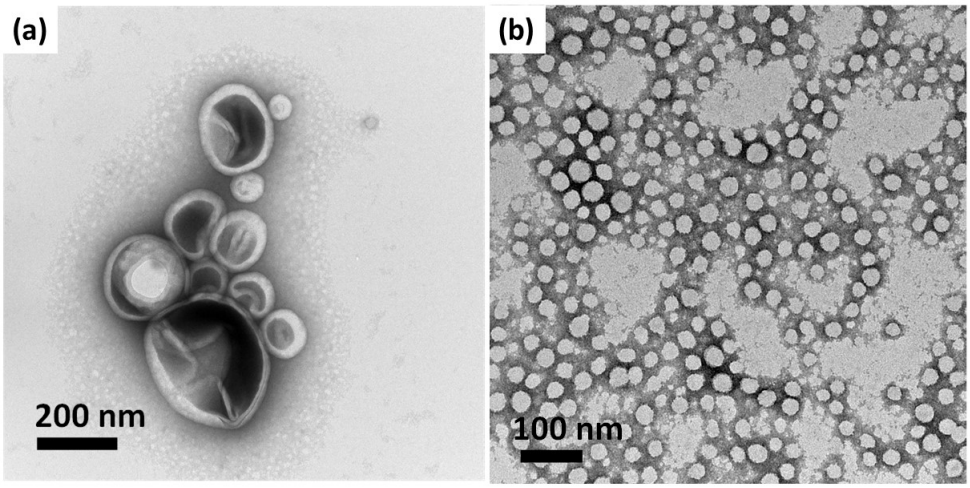

Figure 2. Transmission electron microscopy (TEM) images of (a) paclitaxel-loaded PEG_{2k}-*b*-PC(AzoOMe) vesicles, and (b) paclitaxel-loaded PEG_{2k}-*b*-PC(Cou) micelles prepared by nanoprecipitation using a 1.2/5.0 w/w paclitaxel/polymer ratio.

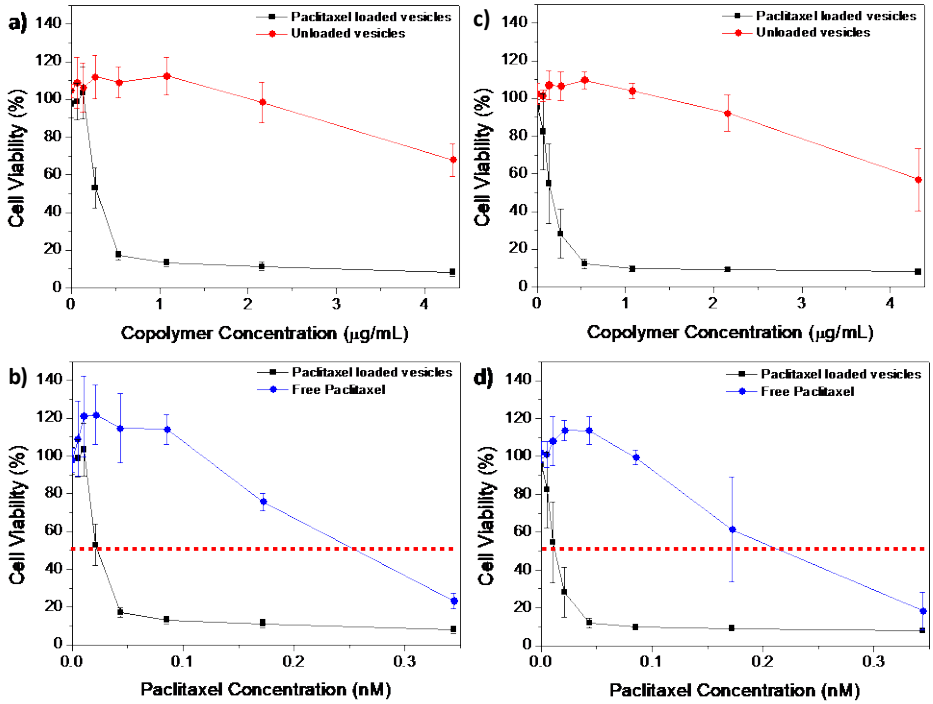

Figure 3. Cell viability in the HeLa cell line after 72 h incubation time (a) with paclitaxel-loaded PEG_{2k}-*b*-PC(AzoOMe) vesicles (black line) or unloaded vesicles (red) at different polymer concentrations (μg mL^{-1}), and (b) with paclitaxel-loaded PEG_{2k}-*b*-PC(AzoOMe) vesicles (black line) or free-paclitaxel (blue) at different paclitaxel concentrations (nM). Effect of light on the cell viability in the HeLa cell line after 24 h incubation time, exposing 10 min to 530 nm light and additional 48 h incubation time (c) with paclitaxel-loaded PEG_{2k}-*b*-PC(AzoOMe) vesicles (black line) or unloaded vesicles (red) at different polymer concentrations (μg mL^{-1}), and (d) with paclitaxel-loaded PEG_{2k}-*b*-PC(AzoOMe) vesicles (black line) or free-paclitaxel (blue) at different PTX concentrations (nM). Dashed red line correspond to half cytotoxic concentration (IC50) defined as the PTX concentration that it is cytotoxic for half of the initial cell population (i.e. cell viability is 50 %), Data represented as mean ± SD, n = 9.

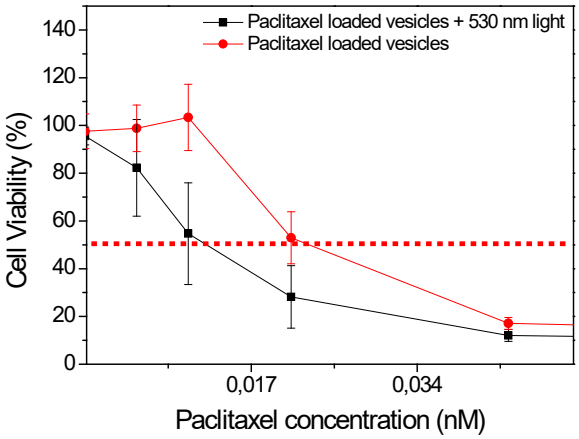

Figure 4. Cell viability of HeLa cell line after 72 h incubation time with paclitaxel-loaded vesicles PEG_{2k}-*b*-PC(AzoOMe) at low PTX concentrations (red line). Cell viability of HeLa cell line after after 24 h incubation time, exposing 10 min to 530 nm light and additional 48 h incubation time (black line) at low PTX concentrations. Dashed red line corresponds to half cytotoxic concentration (IC50) defined as the paclitaxel concentration that it is cytotoxic for half of the initial cell population (i.e. cell viability is 50 %). Data represented as mean ± SD, n = 9.

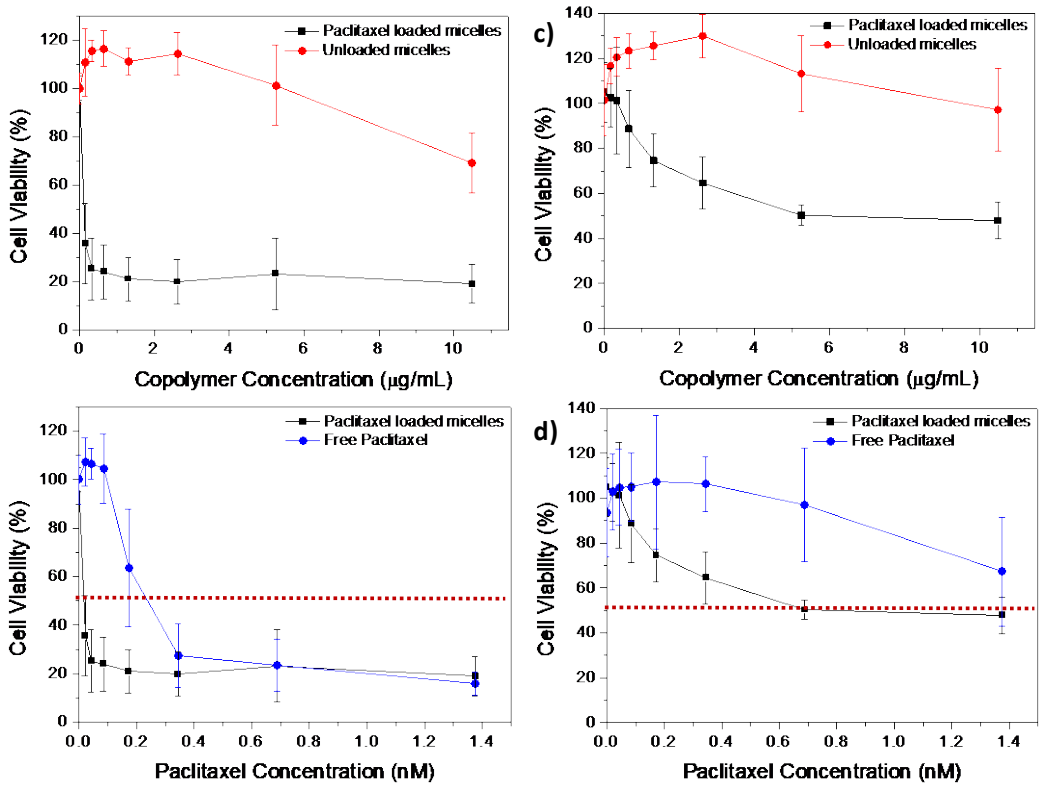

Figure 5. Cell viability in the HeLa cell line after 72 h incubation time (a) with paclitaxel-loaded PEG_{5k}-*b*-PC(Cou) micelles (black line) or unloaded micelles (red) at different polymer concentrations (µg mL^{-1}), and (b) with paclitaxel-loaded PEG_{5k}-*b*-PC(Cou) micelles (black line) or free-paclitaxel (blue) at different paclitaxel concentrations (nM). Cell viability in the Huh-5-2 cell line after 72 h incubation time (c) with paclitaxel-loaded PEG_{5k}-*b*-PC(Cou) micelles (black line) and unloaded micelles (red) at different polymer concentrations (µg mL^{-1}), and (d) with paclitaxel-loaded PEG_{5k}-*b*-PC(Cou) micelles (black line) and free-paclitaxel (blue) at different paclitaxel concentrations (nM). Dashed red line correspond to half cytotoxic concentration (IC50) defined as the PTX concentration that it is cytotoxic for half of the initial cell population (i.e. cell viability is 50 %). Data represented as mean ± SD, n = 9.

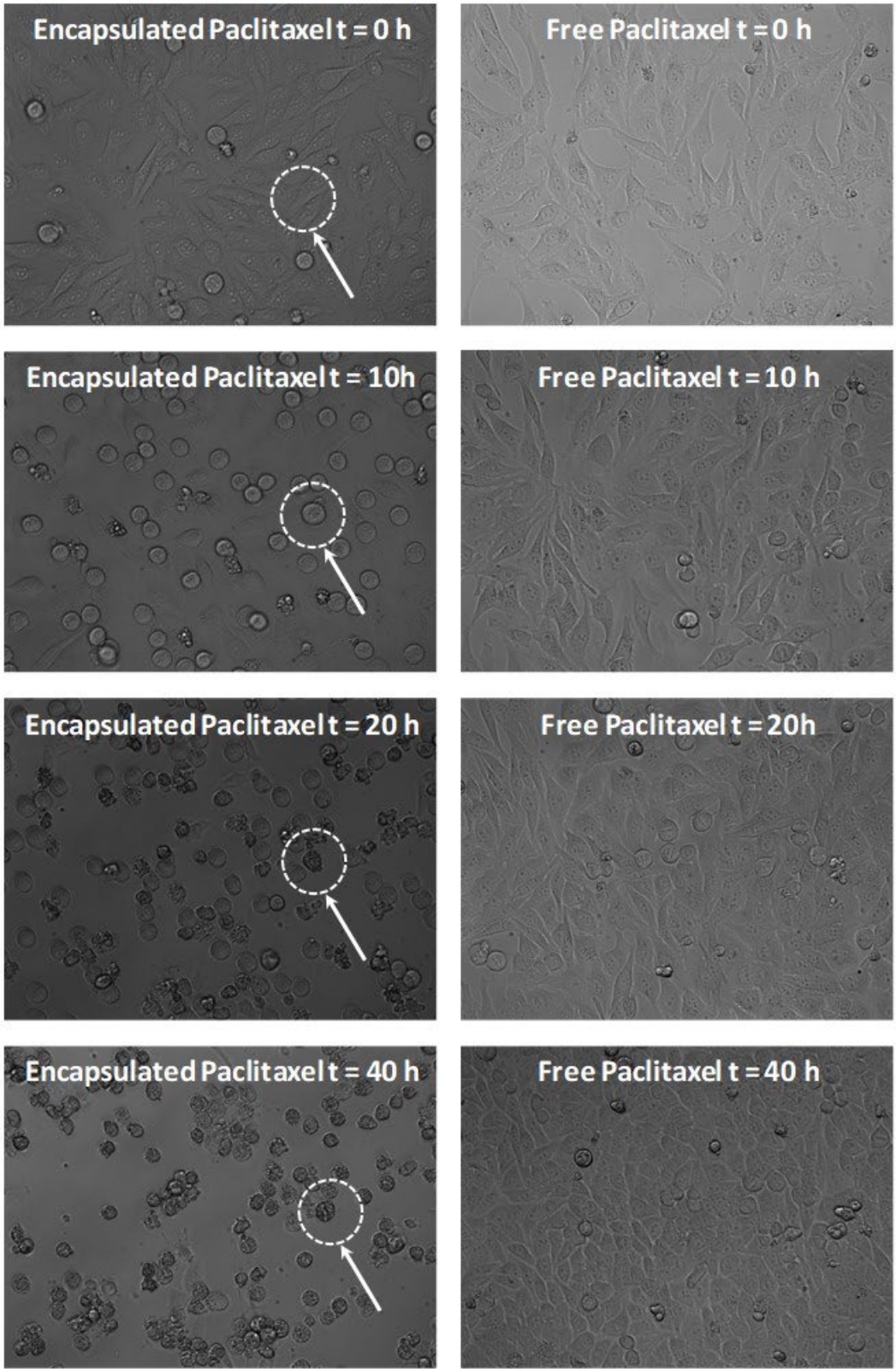

Figure 6. Morphology evaluation of HeLa cell line incubated at different times with paclitaxel (0.02 nM concentration) by time lapse studies in a bright field microscope. (Left) HeLa cell incubated with encapsulated paclitaxel using paclitaxel-loaded PEG_{5k}-*b*-PC(Cou) micelles (0.16 μg mL^{-1} polymer concentration). (Right) HeLa cell line

incubated with free-paclitaxel. Areas where changes are well defined are pointed showing cells detached from the plate at 10 h and apoptotic cells at 20 and 40 h.

Figure 1. Chemical structure of the investigated poly(ethylene glycol)-*b*-polycarbonates (PEG-*b*-PC) containing light-responsive units, either 2,2′,5,5′-tetramethoxyazobenzene (AzoOMe) or [7–(diethylaminocoumarin)–4–yl]methyl ester (Cou) units, in the polycarbonate hydrophobic block.

Figure 2. Transmission electron microscopy (TEM) images of (a) paclitaxel-loaded PEG_{2k}-*b*-PC(AzoOMe) vesicles, and (b) paclitaxel-loaded PEG_{2k}-*b*-PC(Cou) micelles prepared by nanoprecipitation using a 1.2/5.0 w/w paclitaxel/polymer ratio.

Figure 3. Cell viability in the HeLa cell line after 72 h incubation time (a) with paclitaxel-loaded PEG_{2k}-*b*-PC(AzoOMe) vesicles (black line) or unloaded vesicles (red) at different polymer concentrations (μg mL^{-1}), and (b) with paclitaxel-loaded PEG_{2k}-*b*-PC(AzoOMe) vesicles (black line) or free-paclitaxel (blue) at different paclitaxel concentrations (nM). Effect of light on the cell viability in the HeLa cell line after 24 h incubation time, exposing 10 min to 530 nm light and additional 48 h incubation time (c) with paclitaxel-loaded PEG_{2k}-*b*-PC(AzoOMe) vesicles (black line) or unloaded vesicles (red) at different polymer concentrations (μg mL^{-1}), and (d) with paclitaxel-loaded PEG_{2k}-*b*-PC(AzoOMe) vesicles (black line) or free-paclitaxel (blue) at different PTX concentrations (nM). Dashed red line correspond to half cytotoxic concentration (IC50) defined as the PTX concentration that it is cytotoxic for half of the initial cell population (i.e. cell viability is 50 %), Data represented as mean ± SD, n = 9.

Figure 4. Cell viability of HeLa cell line after 72 h incubation time with paclitaxel-loaded vesicles PEG_{2k}-*b*-PC(AzoOMe) at low PTX concentrations (red line). Cell viability of HeLa cell line after after 24 h incubation time, exposing 10 min to 530 nm light and additional 48 h incubation time (black line) at low PTX concentrations. Dashed red line corresponds to half cytotoxic concentration (IC50) defined as the paclitaxel concentration that it is cytotoxic for half of the initial cell population (i.e. cell viability is 50 %). Data represented as mean ± SD, n = 9.

Figure 5. Cell viability in the HeLa cell line after 72 h incubation time (a) with paclitaxel-loaded PEG_{5k}-*b*-PC(Cou) micelles (black line) or unloaded micelles (red) at

different polymer concentrations (μg mL^{-1}), and (b) with paclitaxel-loaded PEG_{5k}-*b*-PC(Cou) micelles (black line) or free-paclitaxel (blue) at different paclitaxel concentrations (nM). Cell viability in the Huh-5-2 cell line after 72 h incubation time (c) with paclitaxel-loaded PEG_{5k}-*b*-PC(Cou) micelles (black line) and unloaded micelles (red) at different polymer concentrations (μg mL^{-1}), and (d) with paclitaxel-loaded PEG_{5k}-*b*-PC(Cou) micelles (black line) and free-paclitaxel (blue) at different paclitaxel concentrations (nM). Dashed red line correspond to half cytotoxic concentration (IC50) defined as the PTX concentration that it is cytotoxic for half of the initial cell population (i.e. cell viability is 50 %). Data represented as mean ± SD, n = 9, * n=7

Figure 6. Morphology evaluation of HeLa cell line incubated at different times with paclitaxel (0.02 nM concentration) by time lapse studies in a bright field microscope. (Left) HeLa cell incubated with encapsulated paclitaxel using paclitaxel-loaded PEG_{5k}-*b*-PC(Cou) micelles (0.16 μg mL^{-1} polymer concentration). (Right) HeLa cell line incubated with free-paclitaxel. Areas where changes are well defined are pointed showing cells detached from the plate at 10 h and apoptotic cells at 20 and 40 h.